Geotechnical Aspects of Underground Construction in Soft Ground – Viggiani (ed)
 ISBN 978-0-415-68367-8

Effect of soil stratification on pipe behaviour due to tunnelling-induced ground movements based on the displacement controlled method

Z.G. Zhang
Department of Civil Engineering, Shanghai University, Shanghai, P.R. China
Department of Geotechnical Engineering, Tongji University, Shanghai, P.R. China
Shanghai Institute of Applied Mathematics and Mechanics, Shanghai, P.R. China

M.S. Huang
Department of Geotechnical Engineering, Tongji University, Shanghai, P.R. China

M.X. Zhang
Department of Civil Engineering, Shanghai University, Shanghai, P.R. China

W.D. Wang
East China Architecture Design Institute, Shanghai, P.R. China

ABSTRACT: The available theoretical predictions for the pipe behaviour due to tunnelling-induced ground movements are usually based on the assumptions that the ground is homogeneous. Actually, effects of soil stratification should be taken into account. This paper presents displacement controlled method to analyze the pipe behaviour due to tunnelling-induced ground movements by the means of layered half space model, which can solve the problem subjected to homogeneous soil as well as multi-layered non-homogeneous soils. The accuracy of the proposed solutions is verified by the centrifuge test data and the results from displacement controlled finite element numerical analysis. In addition, the difference between homogeneous and non-homogeneous layered soils is also studied to estimate the pipe behaviour. The results discussed in this paper indicate that the soil non-homogeneity, neglected in previous solutions, has a significant influence on the existing pipe behavior induced by adjacent tunnelling in multi-layered soils.

1 INTRODUCTION

Underground construction, including tunnelling, causes both vertical and lateral ground movements. For existing buried structures, such as pipes, the ground movements induced by tunnelling may cause reduction in bearing capacity of the structures as well as the development of additional settlements, and lateral movements. Accurate prediction of tunnelling effects on existing buried pipes poses a major challenge during design and practice in the urban geotechnical environments.

The conventional approach for solving the above mentioned problem utilizes the numerical simulation method, such as the finite element method (e.g., Yamaguchi et al., 1998; Addenbrooke and Potts, 2001; Chehade and Shahrour, 2008). Tunnelling in the finite element models is usually simulated by applying forces corresponding to a fraction of the initial stress-state, to the nodes on the tunnel boundary. This method, designated here as the force controlled method (i.e., FCM), has the advantage of being able to take full account of the nonlinear interaction between the existing pipes and its surrounding soil, and to consider the complicated process of tunnelling. However, the FCM will lead to long CPU times since the simulation of the process may be slow. And it is difficult to reflect visually the arbitrary ground loss, which is the main cause for the deformation behavior of existing pipes induced by tunnelling. In order to overcome those disadvantages, the displacement controlled method (i.e., DCM) is applied in this study. In the DCM, the effect of tunnelling is simulated by prescribing displacements up to nodes around the tunnel rather than by adding forces.

Recently some attempts have been made to develop displacement controlled methods to analyze the pipe deformation behaviour due to adjacent tunnelling, all of which are based on the Winkler model or the homogeneous half space model. The conventional approach for obtaining a solution for this problem utilizes the Winkler model such as that proposed by Attewell et al. (1986). The Winkler model has the advantage of simplicity for the complex tunnel-soil-pipe interaction through a single degree of freedom load-displacement relation. However, the Winkler model can not take account of the soil continuum. Klar et al. (2005) obtained a closed form solution for the Winkler model, and suggested a more rigorous solution based on the homogeneous half space model. In this study, the green-field soil settlements are described by a Gaussian curve. Vorster et al. (2005) utilized the boundary integral method to formulate a design method for estimating the effect of tunnelling on buried pipes. They took advantage of the explicitly defined green-field settlements and introduced a modified Gaussian curve which allows the practitioner more freedom in fitting green-field settlement data relatively to the commonly used Gaussian curve. It is worth noting that all of the above solutions are based on the assumption that the ground is homogeneous and the effects of soil stratification should be taken into account.

In the current research, the displacement controlled method is presented to evaluate the effects of soil stratification on pipe behaviour due to tunnelling-induced ground movements. The fundamental solution for the layered soils is obtained by applying the double Laplace transform and transfer matrix method based on the layered half space model. In order to simulate the real non-uniform soil deformation behaviour at the tunnel opening, the displacement controlled pattern proposed by Loganathan and Poulos (1998) is applied to describe green-field soil settlements.

2 LAYERED HALF SPACE MODEL

As shown in Figure 1, the layered half space model is built in a Cartesian coordinate system, and the arbitrary load is concentrated at a point (x_0,y_0,h_{m1})

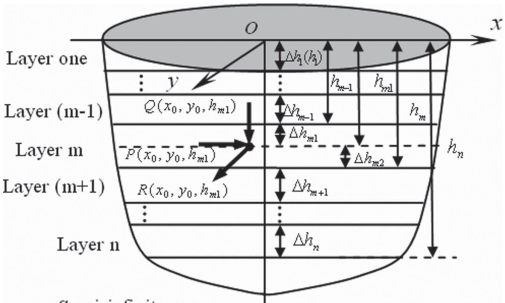

Figure 1. Layered half space model.

in the m th layer (assuming the load surface is considered as an artificial interface). The arbitrary load can be decomposed into the three components $P(x,y_0,h_{m1})$, $R(x_0,y_0,h_{m1})$, and $Q(x_0,y_0,h_{m1})$ along the x, y, z direction, respectively. The key assumptions involved in the derivation are: (1) The layered soils consist of n parallel, elastic isotropic layers lying on a homogeneous elastic half space, where n is an integer and satisfies $n \geq 1$; (2) The i th layer occupies a layer region $h_{i-1} \leq z \leq h_i$ of thickness Δh_i, ($\Delta h_i = h_i - h_{i-1}$), Young's modulus E_i and Poisson's ratio μ_i, where $i = 1, 2, ...,$ or n, and h_0 is defined by the value of zero; (3) the stresses and the displacements located at the each interface between two connected layers are completely continuous; (4) The boundary surface $z = 0$ is considered as traction free.

Considering a traction free condition at the ground surface of the layered system, it can be expressed as follows:

$$\tau_{zx}(x,y,0) = \tau_{zy}(x,y,0) = \sigma_z(x,y,0) = 0 \tag{1}$$

On the other hand, for a fixed boundary condition at the bottom of the layered system (h_n approaches ∞), it can be expressed as follows:

$$u(x,y,h_n) = v(x,y,h_n) = w(x,y,h_n) = 0 \tag{2}$$

According to assumption 3, the continuity conditions at the interfaces of the n-layered system (including the load surface) can be obtained:

$$u(x,y,h_i^+) = u(x,y,h_{i-1}^-) \tag{3a}$$

$$v(x,y,h_i^+) = v(x,y,h_{i-1}^-) \tag{3b}$$

$$w(x,y,h_i^+) = w(x,y,h_{i-1}^-) \tag{3c}$$

$$\tau_{zx}(x,y,h_i^+) = \tau_{zx}(x,y,h_{i-1}^-) - p(x,y,h_{m1})g(z) \tag{3d}$$

$$\tau_{zy}(x,y,h_i^+) = \tau_{zy}(x,y,h_{i-1}^-) - r(x,y,h_{m1})g(z) \tag{3e}$$

$$\sigma_z(x,y,h_i^+) = \sigma_z(x,y,h_{i-1}^-) - q(x,y,h_{m1})g(z) \tag{3f}$$

where h_i is the distance from the bottom of the i th layer to the surface of the first layer ($i = 2, 3, \cdots,$ or n); the superscripts "+" and "−" denote the values of the functions just on upper and lower interface boundary of the i th layer; $p(x,y,h_{m1})$, $r(x,y,h_{m1})$, and $q(x,y,h_{m1})$ denotes the surface density distribution of the point load $P(x_0,y_0,h_{m1})$, $R(x_0,y_0,h_{m1})$, and $Q(x_0,y_0,h_{m1})$, respectively, i.e.,

$$p(x,y,h_{m1}) = P(x_0,y_0,h_{m1})\delta(x-x_0,y-y_0) \tag{4a}$$

$$r(x,y,h_{m1}) = R(x_0,y_0,h_{m1})\delta(x-x_0,y-y_0) \tag{4b}$$

$$q(x,y,h_{m1}) = Q(x_0,y_0,h_{m1})\delta(x-x_0,y-y_0) \tag{4c}$$

with $\delta(x-x_0, y-y_0)$ is the Dirac singularity function; and g(z) is a term to judge whether the arbitrary load existed at the artificial interface or not, i.e.,

$$g(z)=\begin{cases}1 & z=h_{m1}\\ 0 & z\neq h_{m1}\end{cases} \tag{5}$$

In order to reduce the partial differential equation into the algebraic equation, the double Laplace integral transform will be applied to the state variables:

$$\bar{f}(\xi,\eta,z)=\int_0^{\infty}\int_0^{\infty} f(x,y,z)e^{-(\xi x+\eta y)}dxdy \tag{6}$$

where ξ, η are the integration parameters for the Laplace transform.

The inverse double Laplace transform can be expressed as follows:

$$f(x,y,z)=-\frac{1}{4\pi^2}\int_{\beta-i\infty}^{\beta+i\infty}\int_{\beta-i\infty}^{\beta+i\infty}\bar{f}(\xi,\eta,z)e^{\xi x+\eta y}d\xi d\eta \tag{7}$$

Using the double Laplace integral transform for the continuity conditions in Eqs.(3a)–(3f) and the transfer matrix method, the equations governing the relations between the six variables at two boundary surfaces $z=0$ and $z=h_n$ can be expressed as follows:

$$\bar{G}(\xi,\eta,h_n^-)=[F_1]\bar{G}(\xi,\eta,0)-[F_2]\{Q\} \tag{8}$$

where $\bar{G}(\xi,\eta,0)$ is the state variable vector located at the surface $z=0$ in the transform domain, i.e.,

$$\bar{G}(\xi,\eta,0)=[\bar{u}(\xi,\eta,0)\quad \bar{v}(\xi,\eta,0)\quad \bar{w}(\xi,\eta,0)$$
$$\bar{\tau}_{zx}(\xi,\eta,0)\quad \bar{\tau}_{zy}(\xi,\eta,0)\quad \bar{\sigma}_z(\xi,\eta,0)]^{\mathrm{T}}$$

and the elements of $\bar{G}(\xi,\eta,h_n^-)$ are the analogous with the ones of $\bar{G}(\xi,\eta,0)$; $[F_1]$ is the global transfer matrix from the first layer to the n th layer; $[F_2]$ is the local transfer matrix from the m th layer to the n th layer; $\{\bar{Q}\}$ is the load vector in the transform domain, i.e.,

$$[F_1]=\Phi(\xi,\eta,\Delta h_n)\Phi(\xi,\eta,\Delta h_{n-1})\cdots\Phi(\xi,\eta,\Delta h_1) \tag{9a}$$

$$[F_2]=\Phi(\xi,\eta,\Delta h_n)\Phi(\xi,\eta,\Delta h_{n-1})\cdots\Phi(\xi,\eta,\Delta h_{m2}) \tag{9b}$$

$$\{Q\}=[0\quad 0\quad 0\quad \bar{p}(x,y,h_{m1})\quad \bar{r}(x,y,h_{m1})\quad \bar{q}(x,y,h_{m1})]^{\mathrm{T}}$$

in which Δh_i, is the thickness of the i th layer with $\Delta h_1=h_1$, $\Delta h_i=h_i-h_{i-1}(i=2, 3, \cdots, \text{or } n)$, and $\Delta h_{m2}=h_m-h_{m1}$; $\Phi(\xi,\eta,z)$ is called the transfer matrix, and $\Phi(\xi,\eta,z)=\exp[zA(\xi,\eta)]$, i.e.,

$$A(\xi,\eta)=\begin{bmatrix} 0 & 0 & -\xi & \frac{1}{G} & 0 & 0\\ 0 & 0 & -\eta & 0 & \frac{1}{G} & 0\\ \frac{\mu}{\mu-1}\xi & \frac{\mu}{\mu-1}\eta & 0 & 0 & 0 & \frac{1-2\mu}{2G(1-\mu)}\\ \frac{2G}{\mu-1}\xi^2-G\eta^2 & \frac{G(1+\mu)}{\mu-1}\xi\eta & 0 & 0 & 0 & \frac{\mu}{\mu-1}\xi\\ \frac{G(1+\mu)}{\mu-1}\xi\eta & \frac{2G}{\mu-1}\eta^2-G\xi^2 & 0 & 0 & 0 & \frac{\mu}{\mu-1}\eta\\ 0 & 0 & 0 & -\xi & -\eta & 0\end{bmatrix}$$

By applying the two boundary conditions of Eqs.(1) and (2), the $\bar{G}(\xi,\eta,0)$ and $\bar{G}(\xi,\eta,h_n^-)$ in Eq. (8) can be determined analytically.

For a given depth z in the i th layer above the horizontal plane on which the load acts (including just on the plane, i.e., $z\leq h_{m1}$), the stresses and displacements in the transform domain can be expressed as follows:

$$\bar{G}(\xi,\eta,z)=[S]\bar{G}(\xi,\eta,0) \tag{10}$$

where

$$[S]=\Phi(\xi,\eta,z-h_{i-1})\Phi(\xi,\eta,\Delta h_{i-1})\cdots\Phi(\xi,\eta,\Delta h_1) \tag{11}$$

For a given depth z in the i th layer below the horizontal plane on which the load acts (i.e., $z>h_{m1}$), the stresses and displacements in the transform domain can be expressed as follows:

$$\bar{G}(\xi,\eta,z)=[S_1]\bar{G}(\xi,\eta,h_n^-) \tag{12}$$

where

$$[S_1]=\Phi(\xi,\eta,z-h_i)\Phi(\xi,\eta,-\Delta h_{i+1})\cdots\Phi(\xi,\eta,-\Delta h_n) \tag{13}$$

Applying the inverse double Laplace transform of Eq. (7) into the solution $\bar{G}(\xi,\eta,z)$ in Eqs.(10) and (12), the elastic solution for stresses and displacements in the multi-layered soils subjected to the vertical load can be obtained. For the special case $P(x_0,y_0,h_{m1})=1$, $R(x_0,y_0,h_{m1})=1$, and $Q(x_0,y_0,h_{m1})=1$, the solution is the fundamental solution for the multi-layered soils subjected to the arbitrary unit point load.

3 DISPLACEMENT CONTROLLED METHOD

Figure 2 shows a schematic diagram of the problem, in which an existing pipe is buried in layered elastic soils. The key assumptions of the computing model are: (1) The existing pipe remains in contact with the surrounding soils; (2) The existing pipe is elastic, homogeneous, and continuous; (3) The presence of the existing pipe does not affect the

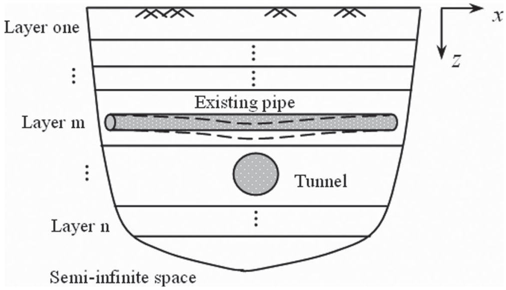

Figure 2. Effects of soil stratification on pipe behaviour due to tunnelling.

tunnel; (4) The soil response to loads, at the pipe level, is not aware of the tunnel; (5) The green-field soil settlements are calculated by analytical solutions proposed by Loganathan and Poulos (1998).

Assumption 3 simply means that the tunnel exhibits the same behavior as it would if there was no pipe. This is an essential assumption in the formulation allowing for decoupling of tunnel behavior in the solution of the pipe response, through the use of a green-field settlement trough. Assumption 4 means that the soils exhibit the same resistance (stiffness) to movement at the pipe level, whether the tunnel exists or not. This assumption allows the use of the fundamental solution for a vertical load in the layered half space model. Assumption 5 shows how to describe the green-field settlement profile at the level of the existing pipe.

Following the above-mentioned assumptions, the pipe behavior is represented by:

$$[K_b]\{u_b\} = \{F_b\} \tag{14}$$

where $[K_b]$ is the stiffness matrix of the tunnel composed of standard beam elements, $\{u_b\}$ is the displacement vector, $\{F_b\}$ is the force vector representing soil loads acting on the beam elements.

The soil continuous displacement at the arbitrary point i can be represented:

$$u_{si} = \sum_{j=1}^{n} R_j \delta_{ij} \tag{15}$$

where R_j is the tunnel force acting on the point j of the soil medium; δ_{ij} is the soil continuous displacement at point i due to the unit load at point j, and it is calculated by the fundamental solution for the layered half space system.

The summation in Eq. (15) can also be written as follows:

$$u_{si} = R_i \delta_{ii} + \sum_{j=1, j\neq i}^{n} R_j \delta_{ij} \tag{16}$$

where the first term of the right side is defined herein as the local displacement due to its own load. The second term is additional continuous displacement at that point due to forces acting at different points. δ_{ii} is the displacement of the singularity point. Such displacement is taken as the average displacement around the circumference of the pipe.

In order to consider the adjacent tunnelling, Eq. (16) can further be decomposed as follows:

$$u_{si} = R_i \delta_{ii} + \sum_{\substack{j=\mathit{first\ pipe\ node} \\ j\neq i}}^{\mathit{last\ pipe\ node}} R_j \delta_{ij} + u_{si}^{f} \tag{17}$$

where the second term of the right side is additional displacement of the point i due to forces resulting from soil-pipe interaction. The third term is additional displacement due to the existence of tunnel. By assumptions 5, u^f_{si} is defined as the green-field settlement profile at pipe level, and is calculated by the method proposed by Loganathan and Poulos (1998).

The static equilibrium condition and the displacement compatibility relation are required. They can be expressed as follows:

$$F_{bi} = -R_i \tag{18}$$

$$u_{si} = u_{bi} = R_i \delta_{ii} + \sum_{\substack{j=\mathit{first\ pipe\ node} \\ j\neq i}}^{\mathit{last\ pipe\ node}} R_j \delta_{ij} + u_{si}^{f} \tag{19}$$

By introducing Eqs.(18) and (19) in to Eq. (14), the deformation behavior of the existing pipe due to tunnelling can be obtained:

$$([K_b]+[K_s]+[K_s][\lambda_s][K_b])\{u_b\} = [K_s]\{u_s^f\} \tag{20}$$

where $[K_s]$ is the local soil stiffness matrix, which only takes consideration of the effect of the singularity point, i.e.,

$$[K_s]_{ij} = \begin{cases} \dfrac{1}{\delta_{ii}} & i = j \\ 0 & i \neq j \end{cases} \tag{21}$$

and $[\lambda_s]$ is the soil flexibility matrix, which doesn't take consideration of the effect of the singularity point, i.e.,

$$[\lambda_s]_{ij} = \begin{cases} \delta_{ij} & i \neq j \\ 0 & i = j \end{cases} \tag{22}$$

in which δ_{ii} and δ_{ij} can be calculated by the inverse transform of Eqs. (10) and (12).

It is worth mentioning that omitting $[K_s][\lambda_s]\ [K_b]$ in the above equation will result in a Winkler model. That means the soil reaction acting on the existing tunnel is not affected by the soil response at different locations along the tunnel. So the term $[K_s][\lambda_s]\ [K_b]$ can thus be regarded as an additional term considering the continuous effects. However, because the components of $[K_s]$ are different from those which are constructed by commonly used subgrade coefficients, such as proposed by Vesic (1961), the solution obtained by omitting this term may not be the Winkler solution.

4 APPLICATION EXAMPLES

By the approach discussed above, the computer program has been written for estimating the existing pipe behavior in the homogeneous soil and layered soils.

4.1 *Example for homogeneous soil*

Vorster (2005) carried out the centrifuge model tests to estimate the effects of tunnelling on existing pipe. The tests were conducted in Leighton Buzzard Fraction E silica sand under 75 g acceleration. In prototype scale, one set of the tests represented a 4.5 m diameter tunnel with a depth of 11.25 m, and running transversely beneath a pipe with the outer diameter 1.2 m and wall thickness 0.15 m (EI = 203.86 MN·m^2) buried at a depth of 4.2 m. And the equivalent average ground loss ratio was set at 0.3%, 1% and 2%, respectively.

The description and analysis of centrifuge model tests is also with prototype scale. In the analysis, the soils are divided into forty layers and each has the same elastic parameters. The thickness of each layer is 1 m. Figures 3 and 4 show calculated pipe vertical displacements and bending moments estimated from the proposed method, together with the observations from centrifuge tests.

From the above figures, it can be seen that the calculated pipe vertical displacements and bending moments are in general consistent with the observed shapes, though there are slightly differences between the two results. When the ground loss ratio is small (e.g., $\varepsilon \leq 1\%$), there is a good agreement between the observed and calculated profiles of the pipe vertical displacements and bending moments in magnitude and shape. However, the difference between the observed and calculated results of the pipe vertical displacement and bending moment profile increases as the ground loss ratio increases. In addition, the difference between the calculated values and observed results in the vicinity of the tunnel (e.g., the range of $x = \pm 5$ m) is obviously. The reason may be that the soil nonlinear effects induced by tunnelling are

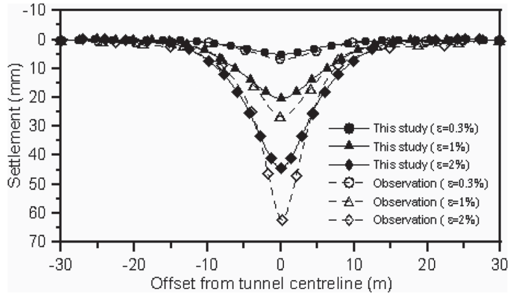

Figure 3. Comparisons of pipe vertical displacement.

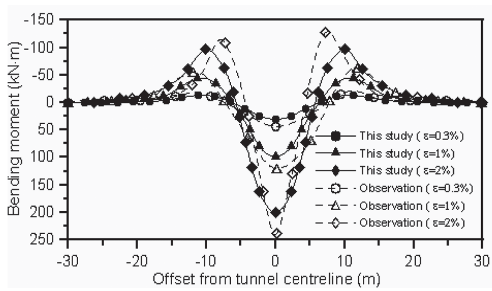

Figure 4. Comparisons of pipe bending moment.

highly when compared with the difference in the field far away from the tunnel and with the difference of the less ground loss ratio.

4.2 *Example for layered soils*

In order to study the effects of the layered complexity on the accuracy of the proposed method, the tunnelling-induced ground movements in five layered soils are analyzed. The first layer is 2.8 m, the Young's modulus is 2.53 MPa, the Poisson's ratio is 0.33; the second layer is 5.2 m, the Young's modulus is 7.44 MPa, the Poisson's ratio is 0.32; the third layer is 12 m, the Young's modulus is 13.16 MPa, the Poisson's ratio is 0.3; the forth layer is 12.1 m, the Young's modulus is 22.3 MPa, the Poisson's ratio is 0.3; the five layer is 20.3 m, the Young's modulus is 50.7 MPa, the Poisson's ratio is 0.2.The outer diameter and inner diameter of an existing tunnel ($EI = 3.09 \times 10^7$ kN·m^2) are 6.2 m and 5.5 m, respectively. It is buried at a depth of 13.3 m. A newly-built tunnel with the outer diameter 6.4 m and axis depth 25 m is running transversely beneath the existing tunnel. The equivalent average ground loss ratio is 2.02%.

In order to compare with the displacement controlled solutions, the finite element numerical analysis is conducted based on the large-scale commercial software. Figure 5 shows the 2-D mesh used in the analysis. There are 5120 elements and 5190 nodes. A displacement controlled finite element model (i.e., DCFEM) proposed by Cheng et al. (2007) is adopted in this study. In this model, the effect of tunnelling is simulated by prescribing displacements to nodes around the tunnel opening rather than by prescribing forces, which is similar to non-uniform oval-shaped ground deformation pattern by Loganathan and Poulos (1998).

Figure 6 show computed green-field soil settlement profiles based on the DCFEM and closed form solutions by Loganathan and Poulos (1998). The numerical results are close to analytical results. Although the maximum settlement from numerical analysis is slightly over analytical results, the difference between the two calculated results in the far field is negligible. Figures 7 and 8 show the existing tunnel settlement and bending moment results using the proposed solutions under the condition of the homogeneous soil and layered soils, and their comparisons with those presented by DCFEM. The elastic parameters of the homogeneous soil are calculated by the means of weighted average method proposed by Poulos and Davis (1980).

As shown in figures 7 and 8, the proposed results based on realistic layered soils provide a reasonably good match with the computed results by DCFEM. However, the proposed results based on homogeneous soil show a poor agreement with DCFEM. The reasons for the slightly differences

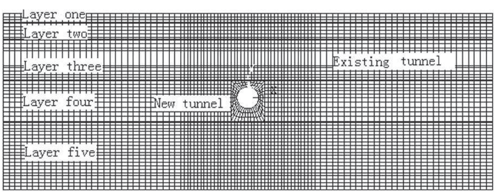

Figure 5. Finite element mesh for five layered soils.

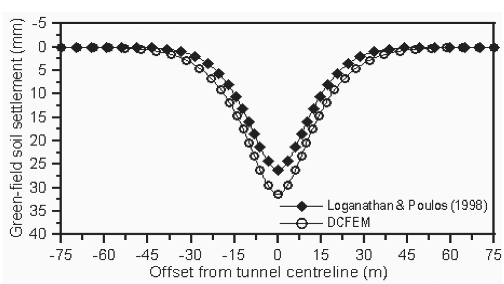

Figure 6. Comparisons of green-field soil settlement.

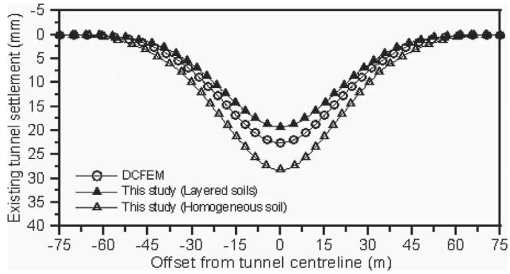

Figure 7. Comparisons of existing tunnel settlement.

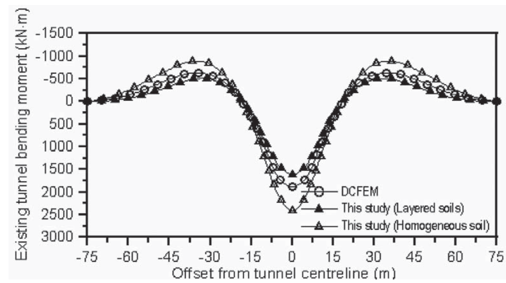

Figure 8. Comparisons of existing tunnel bending moment.

between the proposed results for layered soils and DCFEM may be partially that the different approach for the green-field soil settlements. That is to say, the proposed results of the existing tunnel deformation will more approach the DCFEM analysis results as if the green-field soil settlements by other method more approach those through DCFEM.

From the above-mentioned analysis, it is shown that the proposed method is a valid approach with higher precision in assessing the existing tunnel behavior in non-homogeneous layered soils. Moreover, as to the layered soils where the difference of elastic parameters among successive layers is large, the error obtained via the weighted average method based on homogeneous half space model is not negligible.

5 CONCLUSION

An efficient and practical displacement controlled method to predict the effects of soil stratification on pipe behaviour due to tunnelling-induced ground movements has been suggested. The fundamental solution for layered soils is obtained by applying the double Laplace transform and transfer matrix method based on the layered half space model. Then the existing pipe is regarded as the Euler-Bernoulli beam. Composing green-field soil settlements caused by the adjacent tunnelling to the existing pipe, the displacements and internal forces from the displacement controlled solution equation are obtained.

The results discussed in this paper indicate that the proposed method provides reliable estimates for the pipe behaviour due to tunnelling-induced ground movements in multi-layered soils. Moreover, it has been demonstrated that as for the layered soils where the differences of elastic parameters among successive layers are large, the error is not negligible, which is obtained employing average elastic parameters based on homogeneous soil converted from layered soils. It should be noted that the major limitation of the proposed method stems from the simplified assumptions of linearity and elasticity. However, it appears to be useful for a preliminary design of tunnels to predict the tunnelling-induced pipe deformation, specially considering that the small ground loss can be obtained though the strict operation and the modern technique.

ACKNOWLEDGEMENTS

The authors acknowledge the financial support provided by China Postdoctoral Science Foundation under research grant No. 20100470677 and by the National Science Fund of China for Distinguished Young Scholars under research grant No. 50825803 and by the research fund for the Doctoral Program of Higher Education of China under research grant No. 20070247066, and wish to express their sincere gratitude to Dr. Klar Assaf at Univ. of Cambridge (Technion-Churchill college exchange postdoctoral researcher) for his insightful suggestion.

REFERENCES

Addenbrooke, T.I. & Potts, D.M. 2001. Twin tunnel interaction: surface and subsurface effects. *International Journal of Geomechanics*, ASCE, 1(2): 249–271.

Attewell, P.B., Yeates, J. & Selby, A.R. 1986. Soil movements induced by tunneling and their effects on pipelines and structures. *London: Blackie & Son Ltd.*: 122–145.

Chehade, F.H. & Shahrour, I. 2008. Numerical analysis of the interaction between twin-tunnels: influence of the relative position and construction procedure. *Tunnelling and Underground Space technology*, 23(2): 210–214.

Cheng, C.Y., Dasari, G.R., Chow, Y.K. & Leung C.F. 2007. Finite element analysis of tunnel-soil-pile interaction using displacement controlled model. *Tunnelling and Underground Space Technology*, 22(4): 450–466.

Klar, A., Vorster, T.E.B., Soga, K. & Mair R.J. 2005. Soil-pipe interaction due to tunnelling: comparison between Winkler and elastic continuum solutions. *Geotechnique*, 55(6): 461–466.

Loganathan, N. & Poulos, H.G. 1998. Analytical prediction for tunneling-induced ground movements in clays. *Journal of Geotechnical and geoenvironmental engineering,* ASCE, 124(9): 846–856.

Poulos, H.G. & Davis, E.H. 1980. Pile foundation analysis and design. *New York: Wiley,* 93–100.

Vesic, A.B. 1961. Bending of beams resting on isotropic elastic solids. *Journal of Engineering Mechanics,* ASCE, 87(2): 35–53.

Vorster, T.E.B. 2005. The effect of tunnelling on buried pipes. *Ph.D. Thesis, U.K.: University of Cambridge.*

Vorster, T.E.B., Klar, A., Soga, K. & Mair R.J. 2005. Estimating the effects of tunneling on existing pipelines. *Journal of Geotechnical and geoenvironmental engineering,* ASCE, 131(11): 1399–1410.

Yamaguchi, I., Yamazaki, I. & Kiritani, Y. 1998. Study of ground-tunnel interactions of four shield tunnels driven in close proximity, in relation to design and construction of parallel shield tunnels. *Tunnelling and Underground Space technology*, 13(3): 289–304.